Inorganic Chemistry

Article

pubs.acs.org/IC

Molecular and Electronic Structure of $Re_2Br_4(PMe_3)_4$

Erik V. Johnstone,[*,†,#] Frederic Poineau,[†] Tanya K. Todorova,[‡] Paul M. Forster,[†] Lasse K. Sørensen,[§] Ignacio Fdez. Galván,[§,∥] Roland Lindh,[§,∥] Kenneth R. Czerwinski,[†] and Alfred P. Sattelberger[†,⊥]

[†]Department of Chemistry, University of Nevada Las Vegas, Las Vegas, Nevada 89154, United States

[‡]Laboratoire de Chimie des Processus Biologiques, UMR 8229 CNRS, UPMC-Paris 6, Collège de France, 11 Place Marcelin Berthelot, 75231 Paris Cedex 05, France

[§]Department of Chemistry-Ångström Laboratory and [∥]Uppsala Center of Computational Chemistry−UC_3, Uppsala University, SE-75120 Uppsala, Sweden

[⊥]Argonne National Laboratory, Argonne, Illinois 60439, United States

Supporting Information

ABSTRACT: The dinuclear rhenium(II) complex $Re_2Br_4(PMe_3)_4$ was prepared from the reduction of $[Re_2Br_8]^{2-}$ with $(n\text{-}Bu_4N)BH_4$ in the presence of PMe_3 in propanol. The complex was characterized by single-crystal X-ray diffraction (SCXRD) and UV−visible spectroscopy. It crystallizes in the monoclinic $C2/c$ space group and is isostructural with its molybdenum and technetium analogues. The Re−Re distance (2.2521(3) Å) is slightly longer than the one in $Re_2Cl_4(PMe_3)_4$ (2.247(1) Å). The molecular and electronic structure of $Re_2X_4(PMe_3)_4$ (X = Cl, Br) were studied by multiconfigurational quantum chemical methods. The computed ground-state geometry is in excellent agreement with the experimental structure determined by SCXRD. The calculated total bond order (2.75) is consistent with the presence of an electron-rich triple bond and is similar to the one found for $Re_2Cl_4(PMe_3)_4$. The electronic absorption spectrum of $Re_2Br_4(PMe_3)_4$ was recorded in benzene and shows a series of low-intensity bands in the range 10 000−26 000 cm^{-1}. The absorption bands were assigned based on calculations of the excitation energies with the multireference wave functions followed by second-order perturbation theory using the CASSCF/CASPT2 method. Calculations predict that the lowest energy band corresponds to the $\delta^* \rightarrow \sigma^*$ transition, while the next higher energy bands were attributed to the $\delta^* \rightarrow \pi^*$, $\delta \rightarrow \sigma^*$, and $\delta \rightarrow \pi^*$ transitions.

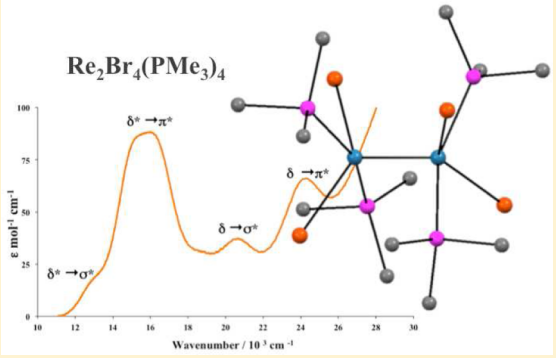

1. INTRODUCTION

The study of dinuclear Re(II) complexes with the stoichiometry $Re_2X_4(PR_3)_4$ (X = Cl, Br, I; PR_3 = tertiary alkyl/aryl phosphine) contributed to the development of metal−metal bond chemistry.[1] Historically, the first halogeno-phosphine Re(II) complexes reported were $Re_2Cl_4(PR_3)_4$ (R_3 = Et_3, $i\text{-}Pr_3$, Et_2Ph, $EtPh_2$, $MePh_2$).[2] These complexes were obtained from the reaction of the $[Re_2Cl_8]^{2-}$ anion with the corresponding trialkyl-phosphine in alcoholic media and were characterized by X-ray diffraction, electrochemical, and spectroscopic methods.[2−5] In $Re_2X_4(PR_3)_4$, the Re_2^{4+} unit exhibits an "electron-rich" triple bond (Figure 1) with a $\sigma^2\pi^4\delta^2\delta^{*2}$ ground-state electronic configuration.[6] Cyclic voltammetry experiments have demonstrated that the Re_2^{4+} unit undergoes two reversible one-electron oxidations to Re_2^{5+} ($\sigma^2\pi^4\delta^2\delta^{*1}$) and Re_2^{6+} ($\sigma^2\pi^4\delta^2$).[7−9] Those redox properties were used in synthetic chemistry, and $[Re_2X_4(PR_3)_4]PF_6$ (X = Cl, Br; R = Me, Et) were obtained from the chemical oxidations of $Re_2X_4(PR_3)_4$ with $NOPF_6$.[3,10] Using this method, the $[Re_2X_4(PMe_3)_4]PF_6$ (X = Cl, Br) salts were recently prepared and the electronic structure of the $[Re_2X_4(PMe_3)_4]^+$ cations was studied by magnetic circular dichroism spectroscopy and theoretical calculations.[11]

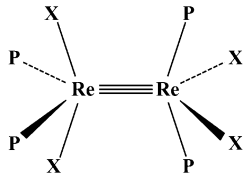

Figure 1. Structural arrangement of $Re_2X_4(PR_3)_4$ complexes with D_{2d} symmetry.

The $Re_2X_4(PMe_3)_4$ (X = Cl, Br, I) dinuclear complexes are fundamental compounds. $Re_2Cl_4(PMe_3)_4$ and $Re_2I_4(PMe_3)_4$ have been extensively studied;[5b,12] the chemistry of $Re_2Br_4(PMe_3)_4$ less so. The latter compound was first reported in 1985 and was characterized by elemental analysis and cyclic voltammetry;[3,9] its crystallographic structure and electronic spectrum have not been reported, and no electronic structure calculations have been performed. Interestingly, its Tc

Received: April 30, 2016
Published: July 7, 2016

DOI: 10.1021/acs.inorgchem.6b01052
Inorg. Chem. 2016, 55, 7111−7116

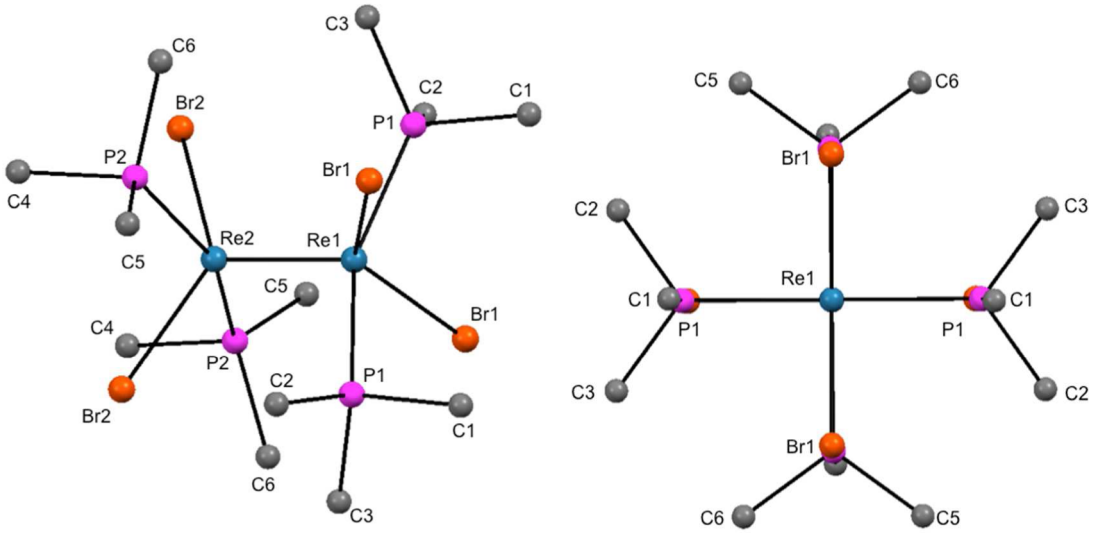

Figure 2. Ball-and-stick representation of $Re_2Br_4(PMe_3)_4$. Color of atoms: C in gray, Re in teal, Br in orange, and P in pink. Hydrogen atoms are omitted for clarity.

homologue, $Tc_2Br_4(PMe_3)_4$, is well-studied from an experimental and theoretical point-of-view.[13]

A combined experimental and theoretical study of $Re_2Br_4(PMe_3)_4$ will provide valuable information relevant to group VII metal−metal bond chemistry; it will inform on the effect of ligand and metal on the electronic structure of the metal−metal bond in $M_2X_4(PMe_3)_4$ (M = Tc, Re; X = Cl, Br) complexes. In this context, we revisited the chemistry of $Re_2Br_4(PMe_3)_4$ and herein report its crystallographic structure. The electronic structures of $Re_2X_4(PMe_3)_4$ (X = Cl, Br) were studied by multiconfigurational quantum chemical methods and compared to the corresponding Tc homologues. The electronic spectrum of $Re_2Br_4(PMe_3)_4$ was recorded in solution, and electronic transitions were assigned based on calculations of the excitation energies with multireference wave functions followed by second-order perturbation theory using the CASSCF/CASPT2 method.

2. EXPERIMENTAL SECTION

Preparation. Reagent-grade solvents, trimethylphosphine (PMe_3, 97%) and $(n\text{-}Bu_4N)_2Re_2Cl_8$ were purchased from Sigma-Aldrich and used as received. The $(n\text{-}Bu_4N)_2Re_2Br_8$ salt was prepared by treating $(n\text{-}Bu_4N)_2Re_2Cl_8$ in warm, concentrated HBr/MeOH and recrystallized as reported in the literature.[14]

$Re_2Br_4(PMe_3)_4$. Using modified procedures reported by Root, et al. and Brant, et al.,[3,4] the compound $(n\text{-}Bu_4N)_2Re_2Br_8$ (1.00 g, 0.650 mmol) was suspended in 10 mL of *i*-PrOH under an argon atmosphere in a 25 mL Schlenk flask charged with a Teflon stir bar and warmed until it was completely dissolved. Trimethylphosphine (460 μL, 5.16 mmol) was added to the suspension via a syringe, and a dark green color was observed. The resulting mixture was then reacted by gently warming. After 5 min, $(n\text{-}Bu_4N)BH_4$ (1.90 g, 7.38 mmol) was added as the solid under ambient conditions, reacted for 10 min, and then quickly cooled to 0 °C. After 1 h, a green precipitate ($Re_2Br_4(PMe_3)_4$, 650.0 mg, yield 61%) was recovered by centrifugation and washed with 3 mL of *i*-PrOH (×2) and 1 mL of hexane (×1). Emerald-green crystals of $Re_2Br_4(PMe_3)_4$ were grown in a week at −25 °C from a toluene/hexane solution (1:2). The crystals were also analyzed in the solid state by single-crystal X-ray diffraction (SCXRD) and in solution by UV−visible spectroscopy (*vide infra*). IR (Figure S1; ATR, ν (cm^{-1})): 2963 (m), 2909 (m), 2874 (m), 2133 (w), 2002 (w), 1612 (w), 1420 (s), 1377 (m), 1292 (s), 1273 (s), 1157 (w), 1064 (vw), 937 (vs), 907 (m), 848 (s), 702 (vw), 729 (s), 667 (s), 594 (w).

Single-Crystal X-ray Diffraction. SCXRD data were collected on a Bruker Apex II system equipped with an Oxford nitrogen cryostream operating at 100 K. Crystals were mounted under Paratone on a glass fiber. Data processing was performed using the Apex II suite of programs, and an absorption correction was performed with SADABS. Structure determination (direct methods) and refinement were carried out using SHELX97.[15]

Spectroscopy. UV−visible spectra were recorded at room temperature in quartz cells (1 cm) on a Cary 6000i double-beam spectrometer. Benzene was used as the reference.

Theoretical Calculations. Quantum chemical calculations were performed using density functional theory (DFT) and multiconfigurational Complete Active Space SCF (CASSCF) method,[16] followed by multistate second-order perturbation theory (MS-CASPT2).[17] Full geometry optimization of the $Re_2X_4(PMe_3)_4$ (X = Cl, Br) dimers was performed at the DFT level employing the hybrid PBE0 exchange−correlation functional[18] with triple-ξ valence plus polarization (def2-TZVP) basis sets on all atoms. A quasi-relativistic pseudopotential was used for the Re atom with 60 core electrons. The TURBOMOLE 6.0 program package was employed.[19] The CASSCF/CASPT2 calculations were performed with the MOLCAS 7.8 package[20] at the DFT-optimized geometries. Relativistic all-electron ANO-RCC basis sets of triple-ζ quality (VTZP) were used for Re, Cl, Br, and P, whereas ANO-RCC basis sets of double-ζ quality (VDZP) were used for C and H.[21] The TZVP basis corresponds to the following contractions: 8s7p5d3f2g1h for Re, 5s4p2d1f for Cl and P, and 6s5p3d1f for Br. The contraction for C and H was 3s2p1d and 2s1p, respectively. Scalar relativistic effects were included using the Douglas−Kroll−Hess Hamiltonian.[22]

In the CASSCF calculations, the complete active space contains 14 electrons in 12 active orbitals (14/12). This space comprises one 5dσ, two 5dπ, and one 5dδ Re−Re bonding orbitals and the corresponding antibonding orbitals and two Re−L σ bonding and the corresponding antibonding orbitals. In the subsequent MS-CASPT2 calculations, orbitals up to and including the 4d for Re, 2p for Cl and P, 3p for Br, and 1s for C were kept frozen. Oscillator strengths were calculated between the perturbed CASSCF states (with MS-CASPT2 energies), employing the so-called dipole moment approximation in the velocity representation, as implemented in the development version of Molcas 8.1.[23−25] The computational costs arising from the two-electron integrals were drastically reduced by employing the Cholesky decomposition (CD) technique[26−28] combined with the local

DOI: 10.1021/acs.inorgchem.6b01052
Inorg. Chem. 2016, 55, 7111−7116

Table 1. Selected Bond Lengths (Å) and Angles (deg) for $Re_2Br_4(PMe_3)_4$

Re(1)−Re(2)	2.2521(3)	P(1)−C(2)	1.816(5)
Re(1)−Br(1)	2.5025(5)	P(1)−C(3)	1.815(5)
Re(1)−P(1)	2.4181(11)	P(2)−C(4)	1.830(5)
Re(2)−Br(2)	2.5051(5)	P(2)−C(5)	1.815(6)
Re(2)−P(2)	2.4210(11)	P(2)−C(6)	1.823(5)
P(1)−C(1)	1.826(5)		
Re(2)−Re(1)−Br(1)	113.936(13)	Re(1)−Re(2)−P(2)[a]	100.98(3)
Re(2)−Re(1)−P(1)	101.13(3)	Br(2)−Re(2)−P(2)[a]	85.43(3)
Br(1)−Re(1)−P(1)	85.30(3)	Re(1)−Re(2)−P(2)	100.98(3)
Br(1)[a]−Re(1)−P(1)	85.72(3)	Br(2)−Re(2)−P(2)	85.67(3)
P(1)−Re(1)−P(1)[a]	157.75(6)	P(2)[a]−Re(2)−P(2)	158.05(6)
Re(1)−Re(2)−Br(2)	114.035(14)	Re(1)−Re(2)−P(2)[a]	100.98(3)
Br(2)[a]−Re(2)−Br(2)	131.93(3)		

[a]Symmetry transformations used to generate equivalent atoms: $-x, y, -z + 1/2$.

Table 2. Average Bond Lengths and Angles for $Re_2X_4(PMe_3)_4$ (X = Cl, Br, I)[a] and $Re_2Br_4(P\text{-}n\text{-}Pr_3)_4$[5b,12]

	distances (Å)			angles (deg)	
system	M−M	M−X	M−P	M−M−X	M−M−P
$Re_2Cl_4(PMe_3)_4$	2.247(1)	2.380(2)	2.417(2)	113.05(6)	102.18(2)
	(2.251)	(2.386)	(2.419)		
$Re_2Br_4(PMe_3)_4$	2.2521(3)	2.504(1)	2.420(2)	113.99(5)	101.06(1)
	(2.250)	(2.535)	(2.430)		
$Re_2Br_4(P\text{-}n\text{-}Pr_3)_4$	2.253(4)	2.579(5)	2.465(9)	105.4(1)	103.3(1)
$Re_2I_4(PMe_3)_4$	2.2541(8)	2.7108(5)	2.427(2)	114.32(5)	102.48(5)
$Tc_2Cl_4(PMe_3)_4$ (ref 13a)	2.1318(2)	2.3858(4)	2.4356(4)	113.28(1)	102.04(1)
	(2.118)	(2.383)	(2.425)		
$Tc_2Br_4(PMe_3)_4$ (ref 13a)	2.1316(5)	2.520(1)	2.441(1)	114.35(1)	102.33(2)
	(2.117)	(2.532)	(2.437)		

[a]The corresponding values for $Tc_2X_4(PMe_3)_4$ (X = Cl, Br) from Ref 13a are given for comparison. Distances computed at the DFT/PBE0/def2-TZVP level are given in parentheses.

exchange (LK) screening.[29] The molecular orbital plots were generated using the Luscus software.[30]

3. RESULTS AND DISCUSSION

Molecular Structure. The $Re_2Br_4(PMe_3)_4$ complex crystallizes in the monoclinic space group $C2/c$ and is isostructural to $M_2X_4(PMe_3)_4$ (M = Tc, Mo, W; X = Cl, Br) and to $Re_2Cl_4(PMe_3)_4$.[13a,31,32] It exhibits D_{2d} symmetry and consists of two eclipsed $ReBr_2(PMe_3)_2$ units linked by a strong Re−Re bond (Figure 2, Table 1). The short Re−Re separation, 2.2521(3) Å, is consistent with the presence of an electron-rich Re−Re triple bond. The Re−Re distance in $Re_2Br_4(PMe_3)_4$ is slightly larger (∼0.005 Å) than in $Re_2Cl_4(PMe_3)_4$, but shorter (∼0.002 Å) than in $Re_2I_4(PMe_3)_4$ (Table 2). Steric effects induced by the halogen ligands are presumably the cause of these differences. The Re−Re separation is similar to the one found in $Re_2Br_4(P\text{-}n\text{-}Pr_3)_4$ (i.e., 2.253(4) Å)[12] and indicates that the nature of the phosphine has a minor effect on the metal−metal separation. The Re−Re separation in $Re_2Br_4(PMe_3)_4$ is 0.12 Å larger than the one in $Tc_2Br_4(PMe_3)_4$. Usually, the metal−metal separations in Re dinuclear complexes are ∼0.1 Å larger than those found in the Tc analogues. Finally, the metal−metal separation in $Re_2Br_4(PMe_3)_4$ is ∼0.03 Å larger than in $(n\text{-}Bu_4N)_2Re_2Br_8$;[33] this difference is due to the absence of a δ bond in $Re_2Br_4(PMe_3)_4$ (*vide infra*).

The average Re−Br (i.e., 2.504(1) Å) and Re−P (i.e., 2.420(2) Å) distances in $Re_2Br_4(PMe_3)_4$ are respectively ∼0.08 and 0.05 Å shorter than in $Re_2Br_4(P\text{-}n\text{-}Pr_3)_4$; these differences are presumably due to steric effects induced by the bulkier phosphine ligand. The Re−P distance in $Re_2Br_4(PMe_3)_4$ is similar to the one found in $Re_2Cl_4(PMe_3)_4$ (i.e., 2.417(2) Å).[12] The Re−Br and Re−P distances are both slightly shorter by ∼0.02 Å than the Tc−Br and Tc−P distances in $Tc_2Br_4(PMe_3)_4$ (Table 2). Similarly, the M−M−Br and M−M−P angles are larger in the Tc complex.[13] Those phenomena may be due to steric effects induced by the shorter metal−metal separation in the Tc complex. There is also the possibility that metal−ligand π-bonding is greater in the rhenium complex than in its technetium analogue.

Geometry optimizations of $Re_2X_4(PMe_3)_4$ (X = Cl, Br), performed at the PBE0/def2-TZVP level of theory, indicate that the calculated Re−Re, Re−X (X = Cl, Br), and Re−P bond distances are in excellent agreement with the experimental values (Table 2). Calculations confirm the experimental observation that the Re−Re bond distance is virtually the same in both $Re_2X_4(PMe_3)_4$ (X = Cl, Br) complexes and longer than the metal−metal bonds in $Tc_2X_4(PMe_3)_4$ and $[Re_2X_8]^{2-}$ dimers by ∼0.13 and 0.03 Å, respectively.[13a,34] The Re−Cl distance is 2.386 Å, whereas Re−Br is significantly longer (i.e., 2.535 Å). The Re−P distances are 2.419 and 2.430 Å in $Re_2Cl_4(PMe_3)_4$ and $Re_2Br_4(PMe_3)_4$, respectively.

Electronic Structure. The CASSCF/CASPT2 calculations were performed in order to investigate the nature of the Re−Re bond in $Re_2X_4(PMe_3)_4$ (X = Cl, Br), and the results are compared with the data published previously for the $Tc_2X_4(PMe_3)_4$ analogues.[13] The CASSCF wave function is analyzed in terms of its natural orbitals and their occupation

DOI: 10.1021/acs.inorgchem.6b01052
Inorg. Chem. 2016, 55, 7111−7116

numbers. The 12 molecular orbitals forming the active space for $Re_2X_4(PMe_3)_4$ (X = Cl, Br) along with their occupation numbers are presented in Figure 3. The dominant electronic

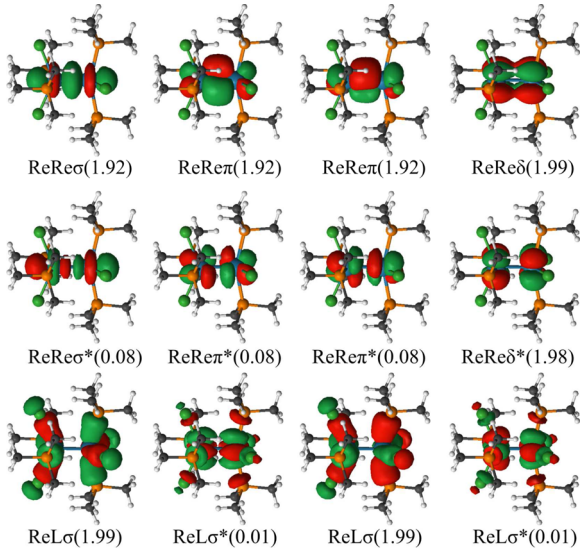

Figure 3. Active orbitals for $Re_2X_4(PMe_3)_4$ (X = Cl, Br) and their occupation numbers in the ground state.

configuration in the $^1A_{1g}$ ground states of $Re_2Cl_4(PMe_3)_4$ and $Re_2Br_4(PMe_3)_4$ has a weight of 88%. The two bonding Re−L orbitals are mainly located on L (L = Cl, Br, and P), while the corresponding antibonding orbitals have a large contribution from the Re $5d_{x^2-y^2}$ orbital. The Re−Re bonding is quantified in terms of effective bond order (EBO), defined as $(\eta b - \eta a)/(\eta b + \eta a)$, where ηb is the occupation number for the bonding natural orbital and ηa is the occupation number for the antibonding natural orbital. The results from the EBO analysis are summarized in Table 3.

Table 3. Effective Bond Order, Total Bond Order, and M−M Distances (DFT/PBE0/def2-TZVP Level) for $M_2X_4(PMe_3)_4$ (M = Re, Tc; X = Cl, Br)[13a]

		effective bond order			
compound	M−M (Å)	σ	π	δ	total bond order
$Re_2Cl_4(PMe_3)_4$	2.251	0.92	1.84	0.01	2.77
$Re_2Br_4(PMe_3)_4$	2.250	0.92	1.84	0.01	2.77
$Tc_2Cl_4(PMe_3)_4$	2.118	0.90	1.81	0.01	2.72
$Tc_2Br_4(PMe_3)_4$	2.117	0.90	1.81	0.01	2.72

The EBO analyses performed for $M_2X_4(PMe_3)_4$ (M = Re, Tc; X = Cl, Br) indicate that the nature of the metal or halogen ligand has only a minor effect on the metal−metal bonding. As evident from Table 3, the σ and π orbitals have similar occupancy, and in turn, the σ and π bonds have approximately the same strength. In $Re_2X_4(PMe_3)_4$, the σ and π EBO values are 0.92 and 1.84, respectively, which are slightly larger than those in $Tc_2X_4(PMe_3)_4$ (i.e., 0.90 and 1.81, respectively). In all the complexes, the occupancy of δ and δ* orbitals is nearly identical, which gives no contribution to the δ bonds. The total bond orders for the $Re_2X_4(PMe_3)_4$ complexes (2.77) are thus only slightly larger than those for the $Tc_2X_4(PMe_3)_4$ analogues (2.72).

The bonding in $Re_2X_4(PMe_3)_4$ can also be compared to the one in $[Re_2X_8]^{2-}$ (Table 4).[34] While the σ components in

Table 4. Effective Bond Order, Total Bond Order, and M−M Distance (CASPT2/ANO-RCC-VTZP Level) for the $[M_2X_8]^{2-}$ (M = Re, Tc; X = Cl, Br)[34]

		effective bond order			
compound	M−M (Å)	σ	π	δ	total bond order
$[Re_2Cl_8]^{2-}$	2.230	0.92	1.76	0.57	3.25
$[Re_2Br_8]^{2-}$	2.210	0.92	1.78	0.62	3.32
$[Tc_2Cl_8]^{2-}$	2.170	0.88	1.68	0.47	3.03
$[Tc_2Br_8]^{2-}$	2.173	0.88	1.69	0.50	3.07

$Re_2X_4(PMe_3)_4$ and $[Re_2X_8]^{2-}$ are identical (i.e., 0.92), the π component is stronger in $Re_2X_4(PMe_3)_4$ than in $[Re_2X_8]^{2-}$ (1.84 vs 1.76, respectively), accounting for a ∼4% increase in the strength of the π bonds. A similar observation has been reported for their technetium analogues, where shortening of the Tc−Tc distance in $Tc_2X_4(PMe_3)_4$ as compared to $[Tc_2X_8]^{2-}$ was associated with significantly stronger π bonds (∼7%).[13a] However, the main difference between $Re_2X_4(PMe_3)_4$ and $[Re_2X_8]^{2-}$ systems is the existence of a weak δ bond (0.57 for X = Cl and 0.62 for X = Br) in $[Re_2X_8]^{2-}$, resulting in a significantly larger total bond order (i.e., 3.25 for $[Re_2Cl_8]^{2-}$ and 3.32 for $[Re_2Br_8]^{2-}$) than in $Re_2X_4(PMe_3)_4$ (i.e., 2.77). Hence, moderate strengthening of the π bonds and absence of δ bonding might be the origin of the longer Re−Re separation in $Re_2X_4(PMe_3)_4$ relative to $[Re_2X_8]^{2-}$.

Electronic Spectroscopy. In order to better understand the electronic structure of $Re_2Br_4(PMe_3)_4$, UV−visible spectroscopy measurements and CASSCF/CASPT2 calculations were performed. Crystals of $Re_2Br_4(PMe_3)_4$ were dissolved in benzene, and the electronic absorption spectrum was recorded. The UV−visible spectrum of $Re_2Br_4(PMe_3)_4$ (Figure 4) shows

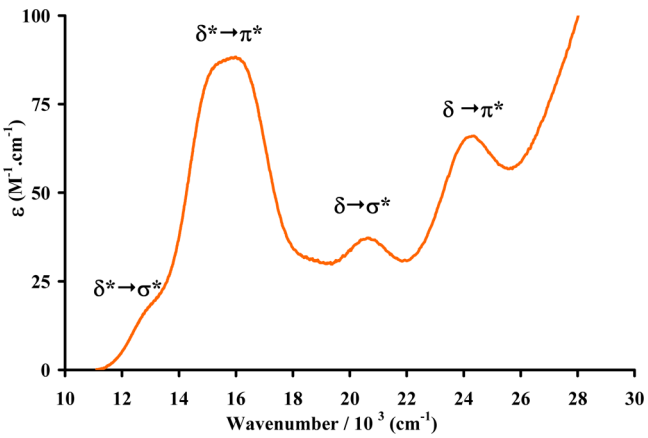

Figure 4. Absorption spectrum of $Re_2Br_4(PMe_3)_4$ in benzene.

a series of four low-intensity bands in the region 10 000−26 000 cm^{-1}. As expected, the transitions in the electronic absorption spectrum of $Re_2Br_4(PMe_3)_4$ (Table 5) are of the same nature as those previously reported for $Tc_2Br_4(PMe_3)_4$, i.e., $\delta^* \rightarrow \sigma^* > \delta^* \rightarrow \pi^* > \delta \rightarrow \sigma^* > \delta \rightarrow \pi^*$. The lowest energy absorption band appears as a shoulder at 13 000 cm^{-1} and could correspond to the dipole forbidden $\delta^* \rightarrow \sigma^*$ transition computed at 13 107 cm^{-1} or to a very weak $\delta^* \rightarrow$

DOI: 10.1021/acs.inorgchem.6b01052
Inorg. Chem. 2016, 55, 7111−7116

Table 5. Experimental Band Maxima (cm^{-1}), Absorption Coefficients ε (M^{-1} cm^{-1}), Assignment, CASPT2 Excitation Energies (cm^{-1}), and Intensities (Using the VTZP Basis Set) for $Re_2Br_4(PMe_3)_4$

experimental	ε	assignment	excitation energy	intensity
13 000	18	$\delta^* \rightarrow \sigma^*$	13 107	DF[a]
		$\delta^* \rightarrow$ ReLσ^*	13 818	$<1.0 \times 10^{-8}$
16 000	88	$\delta^* \rightarrow \pi^*$	17 104	0.02
20 620	37	$\delta \rightarrow \sigma^*$	19 040	$<1.0 \times 10^{-8}$
24 240	66	$\delta \rightarrow \pi^*$	24 281	0.001

[a]DF = dipole-forbidden transition.

ReLσ^* transition (13 818 cm^{-1}), in which the antibonding Re−L orbitals have a dominant contribution from the Re $5d_{x^2-y^2}$ orbital. The strongest absorption (ε = 88 M^{-1} cm^{-1}) is observed at 16 000 cm^{-1} and is assigned to the dipole-allowed $\delta^* \rightarrow \pi^*$ transition. Its excitation energy is computed at 17 104 cm^{-1}. The next band is attributed to the $\delta \rightarrow \sigma^*$ transition, and its calculated position (19 040 cm^{-1}) matches well with the experimental value (20 620 cm^{-1}). The experimental positions of the $\delta^* \rightarrow \sigma^*$ and $\delta \rightarrow \sigma^*$ transitions permit an estimation of the separation between the δ and δ^* orbitals (i.e., 0.95 eV). A similar calculation for $Tc_2Br_4(PMe_3)_4$ indicates that the separation between the δ and δ^* orbitals is 0.65 eV.[13] Finally, the band at 24 240 cm^{-1} is assigned to the $\delta \rightarrow \pi^*$ transition, which is allowed for molecules with D_{2d} symmetry. The positions of the $\delta \rightarrow \pi^*$ and $\delta^* \rightarrow \pi^*$ transitions also permit an estimation of the separation between the δ and δ^* orbitals (i.e., 1.03 eV). In a similar way, the estimated energy between the δ and δ^* orbitals for $Tc_2Br_4(PMe_3)_4$ is 0.68 eV. These results indicate a stabilization of the δ orbital and a destabilization of the δ^* orbital in $Re_2Br_4(PMe_3)_4$ relative to $Tc_2Br_4(PMe_3)_4$.

4. CONCLUSION

The $Re_2Br_4(PMe_3)_4$ complex was synthesized from the reduction of $[Re_2Br_8]^{2-}$ with $(n\text{-}Bu_4N)BH_4$ in the presence of PMe_3 in 2-propanol. The molecular and electronic structure and the electronic spectrum of $Re_2Br_4(PMe_3)_4$ were studied by experimental and theoretical methods. $Re_2Br_4(PMe_3)_4$ crystallizes in the monoclinic $C2/c$ space group and is isostructural with its Mo and Tc analogues. The Re−Re distance in $Re_2Br_4(PMe_3)_4$ is slightly larger than in $Re_2Cl_4(PMe_3)_4$, but shorter than in $Re_2I_4(PMe_3)_4$. The Re−Re separation is similar to the one found in $Re_2Br_4(P\text{-}n\text{-}Pr_3)$ and indicates that the nature of the phosphine ligand weakly influences the metal−metal bond.

The calculated molecular structures of $Re_2X_4(PMe_3)_4$ (X = Cl, Br) are in excellent agreement with the structures determined experimentally. Effective bond order analyses of the σ, π, and δ components in $M_2X_4(PMe_3)_4$ (M = Tc, Re; X = Cl, Br) indicate that the nature of the metal or halogen ligand has a minor effect on the metal−metal bonding. In all complexes, the σ and π orbitals have the same occupancy, and in turn, the σ and π bonds have approximately the same strength, while the occupancy of δ and δ^* orbitals is nearly identical, giving no contribution to the δ bond. In $Re_2X_4(PMe_3)_4$, the σ and π components are slightly stronger than those in $Tc_2X_4(PMe_3)_4$, resulting in a slightly larger total bond order value. This is likely a reflection of the greater radial extension and overlap of the π-bonds in the rhenium(II) dimer. The bonding in $Re_2X_4(PMe_3)_4$ was also compared to the ones in the $[Re_2X_8]^{2-}$. While the σ components are identical, the π component is stronger in $Re_2X_4(PMe_3)_4$ than in $[Re_2X_8]^{2-}$, accounting for a ∼4% increase in the strength of the π bonds. However, the $[Re_2X_8]^{2-}$ complexes have a strong δ bond, giving rise to significantly larger total bond orders as compared to the ones in $Re_2X_4(PMe_3)_4$. The electronic spectrum of $Re_2Br_4(PMe_3)_4$ was recorded in benzene and shows a series of four low-intensity bands in the range 10 000−26 000 cm^{-1}. Assignment of the bands was performed at the CASSCF/CASPT2 level of theory, with an excellent agreement between the computed excitation energies and the experimental band positions. Calculations predict that the lowest energy band corresponds to the $\delta^* \rightarrow \sigma^*$ transition, while the energetically consecutive bands are attributed to $\delta^* \rightarrow \pi^*$, $\delta \rightarrow \sigma^*$, and $\delta \rightarrow \pi^*$ transitions.

Notably, the complex $Re_2F_4(PMe_3)_4$ is still unknown, although it should be accessible using a route similar to the one reported for $Mo_2F_4(PMe_3)_4$.[35] Current work in our laboratory is focused on the preparation of $Re_2F_4(PMe_3)_4$, and the results will be reported in due course.

■ ASSOCIATED CONTENT

Supporting Information

The Supporting Information is available free of charge on the ACS Publications website at DOI: 10.1021/acs.inorgchem.6b01052.

Crystallographic data for $Re_2Br_4(PMe_3)_4$ (CIF)
Crystallographic data for $Re_2Br_4(PMe_3)_4$ (PDF)

■ AUTHOR INFORMATION

Corresponding Author

*E-mail: E.johnstone@sheffield.ac.uk.

Present Address

[#]Department of Materials Science and Engineering, University of Sheffield, Sheffield S1 3JD, U.K.

Funding

Funding for this research was provided by a SISGR grant from the U.S. Department of Energy under contract no. 47824B. R.L., I.F.G., and L.K.S. acknowledge financial support from the Swedish Research Council (Grant No. 2012-3910), the eSSENCE Project, Uppsala University, and the Knut and Alice Wallenberg Foundation (Grant No. KAW-2013.0020).

Notes

The authors declare no competing financial interest.

■ ACKNOWLEDGMENTS

The authors thank Trevor Low and Julie Bertoia for outstanding laboratory support and Prof. Laura Gagliardi for the insightful discussions and contributions.

■ REFERENCES

(1) Cotton, F. A.; Murillo, C. A.; Walton, R. A. *Multiple Bonds between Metal Atoms*, 3rd ed.; Springer: New York, 2005; Chapter 8.
(2) Ebner, J. R.; Walton, R. A. *Inorg. Chem.* **1975**, *14*, 1987−1992.
(3) Root, D. R.; Blevins, C. H.; Lichtenberger, D. L.; Sattelberger, A. P.; Walton, R. A. *J. Am. Chem. Soc.* **1986**, *108*, 953−959.
(4) Brant, P.; Walton, R. A. *Inorg. Chem.* **1978**, *17*, 2674−2677.
(5) (a) Glicksman, H. D.; Walton, R. A. *Inorg. Chem.* **1978**, *17*, 3197−3202. (b) Angaridis, P.; Cotton, F. A.; Dikarev, E. V.; Petrukhina, M. A. *Polyhedron* **2001**, *20*, 755−765.
(6) Bursten, B. E.; Cotton, F. A.; Fanwick, P. E.; Stanley, G. G.; Walton, R. A. *J. Am. Chem. Soc.* **1983**, *105*, 2606−2611.

DOI: 10.1021/acs.inorgchem.6b01052
Inorg. Chem. 2016, 55, 7111−7116

(7) Cotton, F. A.; Pedersen, E. *J. Am. Chem. Soc.* **1975**, *97*, 303−308.
(8) Brant, P.; Salmon, D. J.; Walton, R. A. *J. Am. Chem. Soc.* **1978**, *100*, 4424−4430.
(9) Conner, K. A.; Gennett, T.; Weaver, M. J.; Walton, R. A. *J. Electroanal. Chem. Interfacial Electrochem.* **1985**, *196*, 69−79.
(10) Cotton, F. A.; Dunbar, K. R.; Falvello, L. R.; Tomas, M.; Walton, R. A. *J. Am. Chem. Soc.* **1983**, *105*, 4950−4954.
(11) Habel-Rodriguez, D.; Poineau, F.; Johnstone, E. V.; Czerwinski, K. R.; Sattelberger, A. P.; Kirk, M. L. *Inorg. Chem.* **2014**, *53*, 1260−1262.
(12) Cotton, F. A.; Jennings, J. G.; Price, A. C.; Vidyasagar, K. *Inorg. Chem.* **1990**, *29*, 4138−4143.
(13) (a) Poineau, F.; Forster, P. M.; Todorova, T. K.; Gagliardi, L.; Sattelberger, A. P.; Czerwinski, K. R. *Inorg. Chem.* **2010**, *49*, 6646−6654. (b) Poineau, F.; Weck, P. F.; Forster, P. M.; Sattelberger, A. P.; Czerwinski, K. R. *Dalton Trans.* **2009**, 10338−10342.
(14) Cotton, F. A.; Curtis, N. F.; Robinson, W. R. *Inorg. Chem.* **1965**, *4*, 1696−1700.
(15) Sheldrick, G. M. *Acta Crystallogr., Sect. A: Found. Crystallogr.* **2008**, *64*, 112−122.
(16) Roos, B. O.; Taylor, P. R.; Siegbahn, P. E. M. *Chem. Phys.* **1980**, *48*, 157−173.
(17) (a) Andersson, K.; Malmqvist, P.-Å.; Roos, B. O. *J. Chem. Phys.* **1992**, *96*, 1218−1226. (b) Finley, J.; Malmqvist, P.-Å.; Roos, B. O.; Serrano-Andrés, L. *Chem. Phys. Lett.* **1998**, *288*, 299−306.
(18) Adamo, C.; Barone, V. *J. Chem. Phys.* **1999**, *110*, 6158−6169.
(19) Ahlrichs, R.; Baer, M.; Haeser, M.; Horn, H.; Koelmel, C. *Chem. Phys. Lett.* **1989**, *162*, 165−169.
(20) Aquilante, F.; De Vico, L.; Ferré, N.; Ghigo, G.; Malmqvist, P.-Å.; Neogrády, P.; Pedersen, T. B.; Pitonak, M.; Reiher, M.; Roos, B. O.; Serrano-Andrés, L.; Urban, M.; Veryazov, V.; Lindh, R. *J. Comput. Chem.* **2010**, *31*, 224−247.
(21) (a) Roos, B. O.; Lindh, R.; Malmqvist, P.-Å.; Veryazov, V.; Widmark, P. O. *J. Phys. Chem. A* **2004**, *108*, 2851−2858. (b) Roos, B. O.; Lindh, R.; Malmqvist, P.-Å.; Veryazov, V.; Widmark, P. O. *J. Phys. Chem. A* **2005**, *109*, 6575−6579.
(22) Hess, B. A. *Phys. Rev. A: At., Mol., Opt. Phys.* **1986**, *33*, 3742−3748.
(23) (a) Malmqvist, P.-Å. *Int. J. Quantum Chem.* **1986**, *30*, 479−494. (b) Malmqvist, P.-Å.; Roos, B. O. *Chem. Phys. Lett.* **1989**, *155*, 189−194.
(24) Bauschlicher, C. W., Jr.; Langhoff, S. R. *Theor. Chim. Acta* **1991**, *79*, 93−103.
(25) Aquilante, F.; Autschbach, J.; Carlson, R. K.; Chibotaru, L. F.; Delcey, M. G.; De Vico, L.; Fdez. Galván, I.; Ferré, N.; Frutos, L. M.; Gagliardi, L.; Garavelli, M.; Giussani, A.; Hoyer, C. E.; Li Manni, G.; Lischka, H.; Ma, D.; Malmqvist, P.-Å.; Müller, T.; Nenov, A.; Olivucci, M.; Pedersen, T. B.; Peng, D.; Plasser, F.; Pritchard, B.; Reiher, M.; Rivalta, I.; Schapiro, I.; Segarra-Martí, J.; Stenrup, M.; Truhlar, D. G.; Ungur, L.; Valentini, A.; Vancoillie, S.; Veryazov, V.; Vysotskiy, V. P.; Weingart, O.; Zapata, F.; Lindh, R. *J. Comput. Chem.* **2016**, *37*, 506−541.
(26) Aquilante, F.; Malmqvist, P.-Å.; Pedersen, T. B.; Ghosh, A.; Roos, B. O. *J. Chem. Theory Comput.* **2008**, *4*, 694−702.
(27) Aquilante, F.; Pedersen, T. B.; Lindh, R.; Roos, B. O.; De Meras, A. S.; Koch, H. *J. Chem. Phys.* **2008**, *129*, 024113.
(28) Aquilante, F.; Gagliardi, L.; Pedersen, T. B.; Lindh, R. *J. Chem. Phys.* **2009**, *130*, 154107.
(29) Aquilante, F.; Pedersen, T. B.; Lindh, R. *J. Chem. Phys.* **2007**, *126*, 194106.
(30) Kovacevic, G.; Veryazov, V. *J. Cheminf.* **2015**, *7*, 16.
(31) Burns, C. J.; Burrell, A. K.; Cotton, F. A.; Haefner, S. C.; Sattelberger, A. P. *Inorg. Chem.* **1994**, *33*, 2257−2264.
(32) (a) Hopkins, M. D.; Schaefer, W. P.; Bronikowski, M. J.; Woodruff, W. H.; Miskowski, V. M.; Dallinger, R. F.; Gray, H. B. *J. Am. Chem. Soc.* **1987**, *109*, 408−416. (b) Cotton, F. A.; Extine, M. W.; Felthouse, T. R.; Kolthammer, B. W. S.; Lay, D. G. *J. Am. Chem. Soc.* **1981**, *103*, 4040−4045.
(33) Huang, H. W.; Martin, D. S. *Inorg. Chem.* **1985**, *24*, 96−101.
(34) Poineau, F.; Gagliardi, L.; Forster, P. M.; Sattelberger, A. P.; Czerwinski, K. R. *Dalton Trans.* **2009**, 5954−5959.
(35) Cotton, F. A.; Wiesinger, K. J. *Inorg. Chem.* **1992**, *31*, 920−925.

DOI: 10.1021/acs.inorgchem.6b01052
Inorg. Chem. 2016, 55, 7111−7116